Noise Reduction Techniques for Bayer-Matrix Images

Ossi Kalevo and Henry Rantanen
Nokia Research Center, Visiokatu 1, 33720 Tampere, Finland

ABSTRACT

In this paper, some arrangements to apply Noise Reduction (NR) techniques for images captured by a single sensor digital camera are studied. Usually, the NR filter processes full three-color component image data. This requires that raw Bayer-matrix image data, available from the image sensor, is first interpolated by using Color Filter Array Interpolation (CFAI) method. Another choice is that the raw Bayer-matrix image data is processed directly. The advantages and disadvantages of both processing orders, before (pre-) CFAI and after (post-) CFAI, are studied with linear, multi-stage median, multistage median hybrid and median-rational filters. The comparison is based on the quality of the output image, the processing power requirements and the amount of memory needed. Also the solution, which improves preservation of details in the NR filtering before the CFAI, is proposed.

Keywords: Noise reduction, Bayer matrix, demosaic, digital filtering, median filter

1. INTRODUCTION

Nowadays, electronic image sensors can be found not only in digital cameras, but also in many other imaging applications (e.g. in mobile devices and toys) [1, 2]. The image sensors are small sized and cost-efficient and they provide reasonable image size and image quality. The image quality can be improved by adding Digital Signal Processing (DSP) techniques to the electronic image capture process [3, 4]. Also cost savings are possible using DSP methods. For example, although Complementary Metal Oxide Silicon (CMOS) image sensors produce more noise than Charge Coupled Device (CCD) image sensors, they still are widely used [5]. The CMOS image sensors are cheaper and they do not consume so much power than the CCD image sensors. Using digital denoising filter the increased noise can be reduced after the image has been captured. On the other hand, these new imaging devices do not consists on so much memory and their processing power can also be limited. Therefore, the DSP algorithms (e.g. denoising) used in the imaging device should be as simple as possible, but still powerful enough to provide the output image with good quality.

One noise reduction method is the correlated double sampling (CDS) [6]. In the CDS, the image sensor captures two images. The first image, with exposure time almost zero, provides the initial charging state of the sensor elements. Subtracting the first image from the second image, taken with normal exposure control, the fixed pattern noise can be reduced. The CDS does not reduce the non-static noise, which arises to the image during the exposure process and in the camera electronics. Therefore, additional NR is also required.

For the comparison of the NR methods described in this paper four different test images were used. The subsampled original test images are shown on the Image Page 1. The first (a) image, 'Plant', represents quite a typical image having some amount of fine details. The second (b) image, 'Tiger', is also quite typical image, but it contains more texture than the 'Plant' image. The third (c) image, 'Gray', is totally flat image, where all pixels have the same gray level value (100). It can be used when the noise attenuation capability of the filters is measured. The last (d) image, 'Docu', is used as an example of document imaging. It contains a lot of sharp edges and originally there are only shades of gray (no colors). It is very difficult image for both the NR and the CFAI methods, since false colors can be easily introduced, when the image is processed.

The 'Tiger'-image is from the image gallery of Adobe® PhotoShop® 6.0 CD. The original image is cropped to Video Graphics Array (VGA) -resolution (640x480) for our testing purpose. The 'Gray'-image has been generated by the authors. The 'Plant'-image and the 'Docu'-image have been captured with a digital camera (Olympus Camedia E-10) by the authors. After capturing the images they have been cropped to 4VGA-resolution and after that they are subsampled to VGA-resolution. In that way the effects of camera noise and CFAI are reduced.

When the original VGA-resolution images have been generated they were needed to be modified for our testing purpose. Reducing the amount of available image data the effect of Bayer-matrix has been simulated. Removing the other color components from the original three-color component image data the one-color component image data has been generated. Adding zero average Gaussian noise with standard deviation eight to all the images the noisy Bayer-

Sensors and Camera Systems for Scientific, Industrial, and Digital Photography Applications III, Morley M. Blouke, John Canosa, Nitin Sampat, Editors, Proceedings of SPIE Vol. 4669 (2002) © 2002 SPIE · 0277-786X/02/$15.00

matrix images are generated. This noise level seems visually quite the same as the maximum noise level of the digital image captured with the CMOS image sensor in normal lightning conditions.

When the processed images are compared to the original images, Mean Absolute Error (MAE) and Mean Square Error (MSE) criteria are used. They are defined as:

$$MAE = \frac{\sum_{y=1}^{n}\sum_{x=1}^{m}\left|i(x,y)-\hat{i}(x,y)\right|}{m\times n} \quad \text{and} \tag{1}$$

$$MSE = \frac{\sum_{y=1}^{n}\sum_{x=1}^{m}\left[i(x,y)-\hat{i}(x,y)\right]^2}{m\times n}, \tag{2}$$

where *i(x, y)* is the original pixel value and *î(x, y)* is the corresponding pixel value of the processed image. The size of the image is m x n.

2. IMAGE PROCESSING CHAIN

In a typical low cost digital camera only one imaging sensor is used. Since the sensor is sensitive only to the amount of light it receives, not to the color of it, the light from the camera lens to the sensor is directed through a Color Filter Array (CFA). The CFA, which is usually used, is called as Bayer-matrix. It consists on red, green and blue color filter elements arranged so, that each sensor element, also called as picture element (pixel), collects only one colored light. The number of pixels capturing green light is 50 %, red light is 25 % and blue light is 25 % of the total amount of pixels. The array of pixels in the Bayer-matrix is shown in Figure 1. Note that the values of m and n are even and so the size of the image is even.

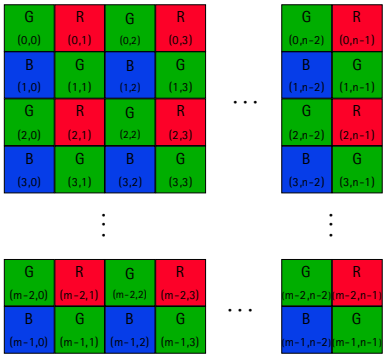

Figure 1: The raw Bayer-Matrix image having m rows and n columns.

For human observer this kind of image is quite useless and the missing color samples in all the three-color components are interpolated by using Color Filter Array Interpolation (CFAI) method, also called as demosaicing method. There are many different CFAI methods available (e.g. bilinear interpolation).

Because the captured image consists on noise, it should also be removed before the output image is ready. Three possible basic image processing chains, including Noise Reduction (NR) and the CFAI are illustrated in Figure 2. The first (a) image processing chain is called as pre-CFAI NR. Here the NR is applied to the raw Bayer-matrix data directly. In this case, the number of pixels to be processed by the NR is the same as the number of pixels in the image. In the second (b) image processing chain, which is called as post-CFAI NR, the order of the NR and the CFAI is swapped. Now, the amount of pixels in the NR is three times the number of pixels in the image. The third (c) image processing chain, in Figure 2, shows the post-CFAI NR arrangement, which is done in the YUV color space. Usually, only the luminance component (Y) is filtered here, because it is the most important component for the Human Visual System (HVS) [7]. This arrangement reduces the number of pixels to be processed to the same number as it was in the first

processing chain. The conversion from RGB color space to YUV color space may not be done unnecessarily. Image compression (e.g. Joint Photographic Experts Group (JPEG)-compression) is usually done in YUV color space, where also the U and V color components are subsampled. Compression is quite often needed when the result image is stored.

The fourth image processing chain, not shown in Figure 2, is to apply the NR method twice. For example, first some pre-CFAI NR method is used in the imaging device and then some post-CFAI NR method is applied in another more powerful device (e.g. in Personal Computer (PC)).

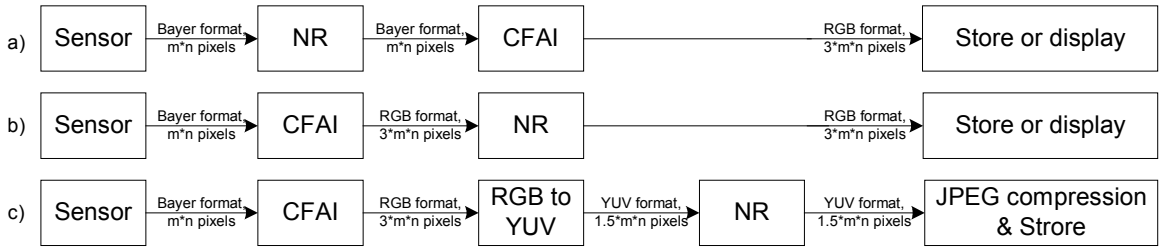

Figure 2: The block diagrams of three different image-processing chains: a) Noise reduction before CFAI, b) noise reduction after CFAI, c) noise reduction after CFAI in YUV.

There were two main elements in the basic image processing chain: the CFAI and the NR. So, the quality of the CFAI algorithm determines also a lot of the quality of the final image. The simplest interpolation methods as pixel copy or bilinear interpolation can destroy the result image too much. There is no need to use very good noise reduction method to preserve sharp details in the image, if these kinds of CFAI methods are used. Small details, thin lines and sharp edges are preserved better when good interpolator (e.g. linear interpolator with Laplacian 2nd order correction terms [8]) is used for the CFAI. This interpolator, later called as 'Laplacian2'-interpolator, is used in the experiments in this paper. The better quality interpolator is used, the better also the improvements in the denoising algorithm can be seen on the final interpolated output image.

In Table 1, interpolation errors caused by pixel copy, bilinear and 'Laplacian2'-interpolator are presented in terms of MAE and MSE. The CFAI errors with the noisy images are presented in Table 2. These two tables show that the error caused by the CFAI method can easily be higher than the error caused by actual sensor noise. The effect of the added noise, having standard deviation of eight, can be seen in Table 2, when the 'Gray'-image is interpolated by the pixel copy CFAI method.

	Pixel copy						Bilinear						Laplacian2					
Image	R_{MAE}	G_{MAE}	B_{MAE}	R_{MSE}	G_{MSE}	B_{MSE}	R_{MAE}	G_{MAE}	B_{MAE}	R_{MSE}	G_{MSE}	B_{MSE}	R_{MAE}	G_{MAE}	B_{MAE}	R_{MSE}	G_{MSE}	B_{MSE}
Gray	0.00	0.00	0.00	0.00	**0.00**	0.00	0.00	0.00	0.00	0.00	**0.00**	0.00	0.00	0.00	0.00	0.00	**0.00**	0.00
Plant	6.01	3.18	6.00	198.99	**102.85**	201.49	3.61	1.87	3.69	66.24	**20.47**	67.07	2.04	1.21	2.38	12.50	**6.02**	15.69
Tiger	9.63	5.74	9.17	393.43	**213.10**	349.16	6.62	3.90	6.52	193.08	**98.75**	183.11	4.07	2.73	3.98	60.78	**47.08**	58.95
Docu	13.22	8.60	13.07	1426.24	**908.33**	1404.96	10.49	5.49	10.51	799.88	**268.01**	799.28	3.19	2.35	3.39	72.32	**59.95**	79.07

Table 1: MSE and MAE of different CFAI methods with the images without noise.

	Pixel copy						Bilinear						Laplacian2					
Image	R_{MAE}	G_{MAE}	B_{MAE}	R_{MSE}	G_{MSE}	B_{MSE}	R_{MAE}	G_{MAE}	B_{MAE}	R_{MSE}	G_{MSE}	B_{MSE}	R_{MAE}	G_{MAE}	B_{MAE}	R_{MSE}	G_{MSE}	B_{MSE}
Gray	6.41	6.39	6.41	64.71	**64.18**	64.55	4.67	4.80	4.72	36.50	**40.23**	36.86	6.31	5.90	6.35	64.50	**55.22**	65.35
Plant	10.08	8.17	9.97	263.19	**166.93**	265.51	6.79	5.79	6.77	102.40	**60.63**	103.03	6.97	6.28	7.06	79.63	**62.97**	81.90
Tiger	12.86	10.11	12.45	455.63	**275.08**	410.21	9.24	7.55	9.16	228.19	**137.96**	218.97	8.09	7.29	8.11	123.65	**102.94**	123.01
Docu	17.11	13.55	17.50	1469.76	**965.58**	1461.93	13.37	9.33	13.73	828.84	**305.89**	832.80	7.36	7.13	7.97	122.52	**111.05**	137.10

Table 2: MSE and MAE of different CFAI methods with the noisy images.

Small capture of the 'Docu'-image without noise and the 'Plant'-image with noise are presented on the Image Page 2 and on the Image Page 3. The effect of using different CFAI methods can be seen from the first three (a - c) images.

2. POST- AND PRE-CFAI NOISE REDUCTION METHODS

When the post-CFAI NR image processing chain is used the image consists on all the three-color component values for each pixel, when the NR is applied. So, the ordinary NR filters can be used for each color components separately. Lowpass (smoothing) spatial filter, also referred as neighborhood averaging, is one very commonly presented NR filter [9, 10]. Usually, this filter is used in 3x3-window mask. This filter can be used with very low memory and also the processing power requirement is low. There are two main problems with this kind of filters. 1) When the size of the filter window is increased the smoothing of the image is also increased rapidly. 2) The processing power requirements and the memory consumption are also increased rapidly, when the size of filter window is increased.

In this paper, low memory and low processing power devices are chosen to be as target devices and so the filter window for the post-CFAI NR chain has been chosen to be 3x3. This causes that the required memory, with the VGA-resolution image, is three-color components for each pixel in three rows (3x3x640 bytes) and the number of processed pixels is 3x480x640.

When the pre-CFAI NR chain is used the image consists on only one-color component value for each pixel, when the NR is processed. Any of the 4-neighbor pixels does not consist the same color component value as the center pixel. So, the size of the filter window has to be increased. If the size of the filter window is 5x5, there are at least as many same color component values as there are in the post-CFAI NR chain, when the 3x3 filter window is used. The increase of filter window does not still change the memory consumption requirements bigger than with the post-CFAI NR chain. Now, there is only one-color component for each pixel available and so only five rows are needed to be in memory (1x5x640 bytes). The number of processed pixels is 1x480x640, which is only one third of the processed pixels in the post-CFAI NR. So, if the filtering methods are equal the processing power requirements should be reduced to one third of the post-CFAI NR requirements.

To find out, how much there is difference in the image quality, when using the pre-CFAI NR and the post-CFAI NR methods some quite common NR algorithms were tested. The used algorithms are described in the following subchapters 2.1, 2.2 and 2.3.

2.1. LINEAR FILTERS

Two linear filter implementations were tested. The first one is called as 'Linear 1'-filter. The weight of the center pixel is 25% of the total weights of filter. In the second one, called as 'Linear 2'-filter, the weight of the center pixel has been increased to 50% of the total weights of filter. Therefore, 'Linear 2'-filter preserves better details than 'Linear 1'-filter whereas 'Linear 1'-filter has better noise reduction capability than 'Linear 2'-filter. The masks of the both filters are presented in Figure 3.

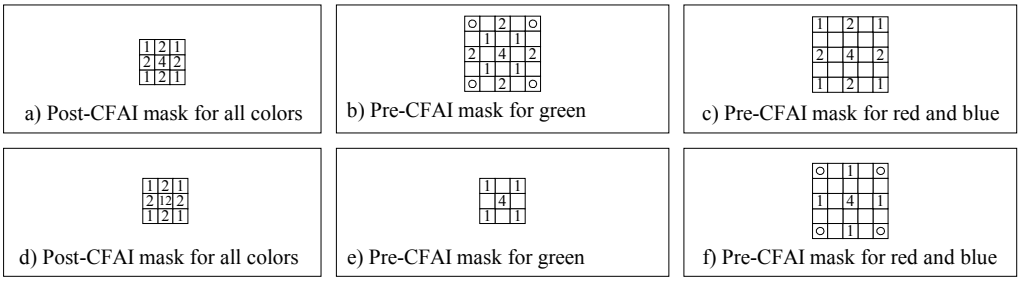

Figure 3: Filter masks for the linear filters: a) - c) The structure of 'Linear 1'-filter, d) – f) the structure of 'Linear 2'-filter. No value in pixel position means there is different color component value in that location.

2.2. MULTISTAGE MEDIAN AND MEDIAN HYBRID FILTERS

Multistage median and median hybrid filters provides more flexibility to the filter design [11, 12]. They take into account the spatial-order information better than the normal median filter. Also the size of the filter window can be larger since it can be divided into smaller subfilter windows. These filters have been proven to preserve two-dimensional structures and to be good smoothers in heavy-tailed noise [13, 14]. So, three different multistage filters have been chosen to use in our tests.

The first multistage median filter, named as 'Median 1'-filter, is a bidirectional filter. It has one '+'-shaped and one 'x'-shaped 5-point median subfilters. The highest stage consists of a 3-point median filter, where the original pixel value is used as the third input.

The other two multistage median filters are using unidirectional linear filters as subfilters. So, they are called as multistage median hybrid filters. In 'Median 1'-filter, there were two 5-point median subfilters used. Now, these subfilters are replaced by two 3-point '+'-shaped and 'x'-shaped median filters. The original pixel value and two unidirectional linear filter values are used as the input values for these 3-point median filters.

The structures of multistage median and multistage median hybrid filters are shown in Figure 4. 'Median 1'-filter is shown in subfigures a) – c). 'Median 3'-filter uses all the pixel values shown in subfigures d) – f), but 'Median 2'-filter does not use the original (center) pixel value, when the average is calculated. Therefore, 'Median 3'-filter preserves details better than 'Median 2'-filter, but 'Median 2'-filter has better noise reduction capability than 'Median 3'-filter.

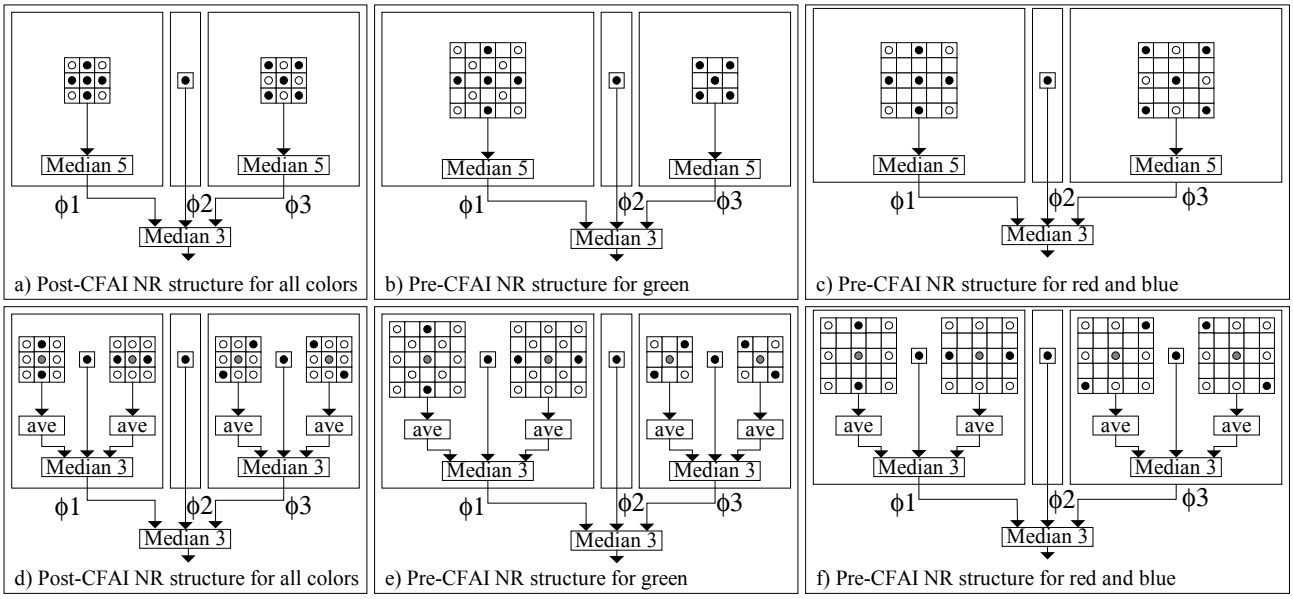

Figure 4: Multistage Median and Median Hybrid filters structures: a) - c) The structure of 'Median 1'- filter, where two bidirectional 5-point median subfilters ('+'-shaped and 'x'-shaped) are used, and d) - f) the structure of 'Median2'-filter and 'Median3'-filter, where the lowest stage subfilters are unidirectional linear filters.

2.3. MEDIAN RATIONAL HYBRID FILTER

Median Rational Hybrid Filters (MRHF) are known to provide good noise attenuation properties whereas on changing areas the noise attenuation is traded for good response to the change [15]. The output value *y(m,n)* of the MRHF is calculated using Equation 3.

$$y(m,n) = \phi 2(m,n) + \frac{\phi 1(m,n) - 2 * \phi 2(m,n) + \phi 3(m,n)}{h + k(\phi 1(m,n) - \phi 3(m,n))}, \qquad (3)$$

where h and k are some positive constants.

The used MRHF, called as 'Rational'-filter, consist of one Center Weighted Median Filter (CWMF) and two 5-point median filters. The shapes of the 5-point median filters ('+'-shaped and 'x'-shaped) are similar as the filters used in 'Median 1'-filter. For the constants, 2 for h and 0.01 for k are used. The structure of the used 'Rational'-filter is shown in Figure 5.

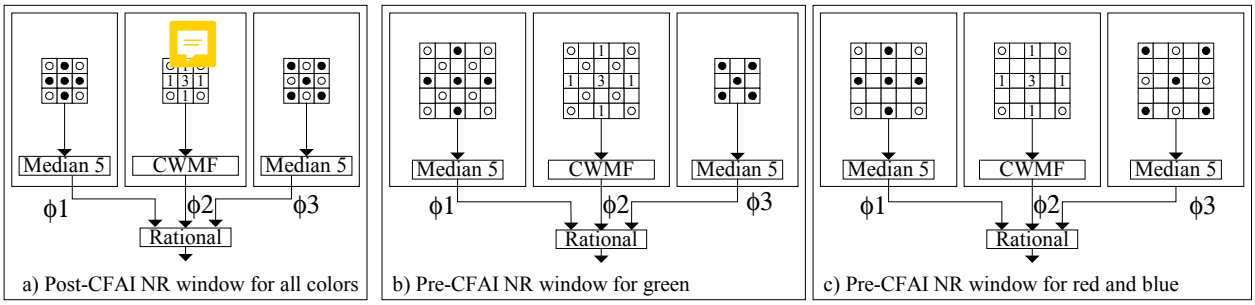

Figure 5: The structure of the MRHF having two subfilters, ϕ1 and ϕ3, where is '+'-shaped and 'x'-shaped masks and the CMWF ϕ2 having '+' shaped mask. The numbers in the CMWF-window denotes the used weights.

2.4. NOISE ELIMINATION CAPABILITY AND IMAGE SMOOTHING

The 'Gray'-image with noise and the 'Docu'-image without noise were processed with six NR filters presented in previous sections 2.1, 2.2 and 2.3. 'Laplacian 2'-method was used for the CFAI. The filtered images were compared to the original images and MAE and MSE were calculated. These error results have shown in Table 3 and in Table 4. Noise reduction capability of the filters can be seen from the 'Gray'-image results. The results of the 'Docu'-image are showing how much these filters destroy edges, lines and fine details. The filtered 'Docu'-images are shown on the Image Page 2. The images d) - f) show results with three post-CFAI NR filters and the images g) - i) show results with the same three pre-CFAI NR filters.

Filter	Post-CFAI NR for 'Gray'						Pre-CFAI NR for 'Gray					
	R_{MAE}	G_{MAE}	B_{MAE}	R_{MSE}	G_{MSE}	B_{MSE}	R_{MAE}	G_{MAE}	B_{MAE}	R_{MSE}	G_{MSE}	B_{MSE}
Linear 1	3.63	3.10	3.75	20.89	**15.20**	21.92	2.36	2.25	2.56	9.08	**8.17**	10.27
Linear 2	4.33	3.85	4.41	29.71	**23.25**	30.65	3.39	3.22	3.51	18.30	**16.61**	19.31
Median 1	4.35	4.03	4.43	29.80	**25.41**	30.81	3.44	3.41	3.55	19.12	**18.43**	20.18
Median 2	4.54	4.20	4.61	32.30	**27.59**	33.29	3.70	3.59	3.81	21.86	**20.27**	22.89
Median 3	5.05	4.69	5.11	39.44	**33.60**	40.40	4.44	4.28	4.51	30.66	**27.89**	31.60
Rational	3.96	3.60	4.06	24.77	**20.42**	25.84	2.76	2.69	2.91	12.37	**11.66**	13.45

Table 3: MAE and MSE of the post-CFAI NR and the pre-CFAI NR calculated by the 'Gray'-image with noise.

Filter	Post-CFAI NR for 'Docu'						Pre-CFAI NR for 'Docu'					
	R_{MAE}	G_{MAE}	B_{MAE}	R_{MSE}	G_{MSE}	B_{MSE}	R_{MAE}	G_{MAE}	B_{MAE}	R_{MSE}	G_{MSE}	B_{MSE}
Linear 1	10.23	9.94	10.33	475.5	**452.7**	478.6	15.08	13.58	15.01	911.6	**769.9**	886.8
Linear 2	7.44	7.02	7.56	249.5	**225.0**	254.1	9.98	9.49	10.12	475.3	**406.3**	478.8
Median 1	5.08	4.37	5.20	212.4	**189.1**	215.6	8.80	7.19	8.83	657.7	**511.5**	641.5
Median 2	4.79	4.12	4.90	169.2	**152.9**	172.5	7.04	5.81	7.12	394.8	**306.5**	386.8
Median 3	4.08	3.41	4.19	113.7	**99.1**	117.9	5.40	4.25	5.51	214.2	**156.9**	212.5
Rational	4.22	3.54	4.41	120.5	**104.0**	127.7	6.86	5.82	6.94	397.6	**331.2**	391.1

Table 4: MAE and MSE of the post-CFAI NR and the pre-CFAI NR calculated by the 'Docu'-image without noise.

Based on the experiment results the pre-CFAI NR filters can eliminate noise much better than the post-CFAI NR filters. On the other hand the post-CFAI NR filters preserve edges and details much better than the pre-CFAI NR filters.

2.5. SOLUTIONS FOR PRE-CFAI NOISE REDUCTION FILTERING

In the previous section 2.4, the smoothing properties of the pre-CFAI NR-filters have been noticed. To improve the edge preservation of the pre-CFAI NR the use of simple detail detection method with limiter is proposed by the authors. The detector tries to detect, when there is edge, line or fine detail around the processed original pixel position. It operates by detecting edges in the 4-neighbors of the current pixel. When green pixel is processed, this neighborhood contains only red and blue pixels, whereas in the red (and in the blue) case, this neighborhood contains only green samples. The used pixels in detection are shown in Figure 6.

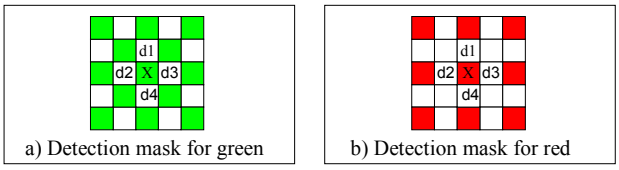

Figure 6: Detail detector: a) Mask for green, b) mask for red.

The detector calculates two absolute differences: vertical *abs(d1 – d4)* and horizontal *abs(d2 – d3)*. If at least the other difference is bigger than the predefined *threshold* an edge is detected. When the edge is detected, the change from the original pixel value to the filtered result value is limited by *limit*. In the other words, the NR filtered value is clipped to between [original – *limit*, original + *limit*], when the edge is detected.

This detection system obviously fails, when the edge is in one color component only. Fortunately, this happens quite rarely in natural images. For example, a change in the luminance level leads to a change in all three-color components. So, luminance level change can be detected with the proposed method, if the change is big enough. The *limit* value used in our experiments was 13 and the *threshold* for edge detection was 6. Both of these values should be changed depending on the noise level of the image.

To find out, how this simple detail detection method with limiter operates, the same images as earlier are processed by all the pre-CFAI NR filters with detector. The error results for both the 'Gray'-image with noise and the 'Docu'-image without noise are shown in Table 5.

Filter	Pre-CFAI NR with detection for 'Gray'						Pre-CFAI NR with detection for 'Docu'					
	R_{MAE}	G_{MAE}	B_{MAE}	R_{MSE}	$\mathbf{G_{MSE}}$	B_{MSE}	R_{MAE}	G_{MAE}	B_{MAE}	R_{MSE}	$\mathbf{G_{MSE}}$	B_{MSE}
Linear 1	2.45	2.31	2.63	10.04	**8.83**	11.11	6.74	5.68	6.80	151.23	**111.32**	153.4
Linear 2	3.39	3.22	3.51	18.37	**16.66**	19.38	5.72	4.86	5.86	125.86	**95.31**	132.4
Median 1	3.52	3.47	3.62	20.05	**19.12**	21.06	4.05	3.26	4.21	92.73	**71.29**	98.03
Median 2	3.77	3.65	3.87	22.68	**20.96**	23.70	3.99	3.15	4.15	91.69	**69.23**	96.41
Median 3	4.45	4.28	4.52	30.79	**27.98**	31.74	3.85	2.99	4.01	88.73	**66.73**	93.84
Rational	2.85	2.77	2.99	13.37	**12.44**	14.41	4.01	3.34	4.14	91.00	**71.63**	95.28

Table 5: MAE and MSE of the pre-CFAI NR with detection calculated by the noisy 'Gray'-image and the 'Docu'-image without noise.

The NR performance is reduced only a little with the 'Gray'-image. But the improvements with the error results of the 'Docu'-image are significant. The improvements in the details can also be easily seen in the processed images on the Image Page 2. The images j) - l) are processed by the pre-CFAI NR filters with detector.

3. EXPERIMENTAL RESULTS

The use of the post-CFAI NR and the pre-CFAI NR methods were discussed in Chapter 2. Also the detail detector for the pre-CFAI NR methods was proposed. The experiments with natural images are shown in this Chapter. Three different images with noise are processed using all the filters presented in Chapter 2. The results of the processed noisy 'Plant', noisy 'Tiger' and noisy 'Docu' images are shown in Table 6, in Table 7 and in Table 8. The filtered noisy 'Plant'-images can be found on the Image Page 2. The images d) – l) show results with NR filters.

Filter	Post-CFAI NR for 'Plant'						Pre-CFAI NR for 'Plant'						Pre-CFAI NR with detection for 'Plant'					
	R_{MAE}	G_{MAE}	B_{MAE}	R_{MSE}	$\mathbf{G_{MSE}}$	B_{MSE}	R_{MAE}	G_{MAE}	B_{MAE}	R_{MSE}	$\mathbf{G_{MSE}}$	B_{MSE}	R_{MAE}	G_{MAE}	B_{MAE}	R_{MSE}	$\mathbf{G_{MSE}}$	B_{MSE}
Linear 1	5.79	4.90	5.81	66.93	**49.80**	68.35	7.72	6.02	7.53	152.68	**91.85**	150.35	5.91	4.86	5.83	69.30	**46.68**	69.04
Linear 2	5.72	4.84	5.77	57.25	**40.47**	59.07	6.10	5.00	6.13	78.50	**50.58**	81.23	5.59	4.65	5.62	58.19	**39.03**	60.13
Median 1	5.63	4.89	5.67	54.35	**39.89**	56.06	5.79	4.83	5.81	70.17	**44.35**	75.41	5.42	4.64	5.44	52.07	**36.21**	53.66
Median 2	5.62	4.88	5.69	54.04	**39.58**	56.47	5.86	4.90	5.88	71.46	**46.77**	75.38	5.45	4.63	5.48	52.40	**35.83**	53.88
Median 3	5.89	5.16	5.98	57.26	**42.54**	59.63	5.81	4.96	5.89	60.91	**41.46**	64.32	5.68	4.89	5.74	54.79	**38.73**	56.96
Rational	5.33	4.55	5.36	49.16	**34.77**	50.29	5.31	4.42	5.25	57.97	**38.66**	59.27	5.06	4.25	5.04	46.87	**31.67**	47.60

Table 6: MAE and MSE of all the presented NR methods with the noisy 'Plant'-image.

Filter	Post-CFAI NR for 'Tiger'						Pre-CFAI NR for 'Tiger'						Pre-CFAI NR with detection for 'Tiger'					
	R_{MAE}	G_{MAE}	B_{MAE}	R_{MSE}	$\mathbf{G_{MSE}}$	B_{MSE}	R_{MAE}	G_{MAE}	B_{MAE}	R_{MSE}	$\mathbf{G_{MSE}}$	B_{MSE}	R_{MAE}	G_{MAE}	B_{MAE}	R_{MSE}	$\mathbf{G_{MSE}}$	B_{MSE}
Linear 1	8.11	7.58	7.92	164.13	**151.21**	152.79	9.86	9.18	9.43	266.28	**240.71**	239.86	7.30	6.62	7.10	115.10	**98.78**	107.79
Linear 2	7.42	6.79	7.28	121.69	**106.03**	114.06	7.89	7.28	7.64	152.39	**134.15**	139.18	6.91	6.30	6.79	102.95	**88.94**	96.95
Median 1	7.69	7.16	7.55	136.03	**124.59**	127.78	8.43	7.75	8.16	190.62	**166.05**	172.60	7.03	6.38	6.90	103.68	**88.06**	97.90
Median 2	7.43	6.93	7.31	121.35	**111.61**	113.80	8.02	7.26	7.77	161.11	**135.28**	145.29	6.98	6.25	6.85	101.36	**84.44**	95.73
Median 3	7.31	6.72	7.23	108.85	**96.42**	103.59	7.45	6.70	7.25	120.24	**99.22**	110.24	7.07	6.34	6.97	101.51	**84.42**	96.30
Rational	7.33	6.75	7.23	122.84	**110.67**	116.74	8.36	7.79	8.14	198.28	**183.55**	185.11	6.87	6.22	6.75	102.85	**88.11**	97.52

Table 7: MAE and MSE of all the presented NR methods with the noisy 'Tiger'-image.

Filter	Post-CFAI NR for 'Docu'						Pre-CFAI NR for 'Docu'						Pre-CFAI NR with detection for 'Docu'					
	R_{MAE}	G_{MAE}	B_{MAE}	R_{MSE}	$\mathbf{G_{MSE}}$	B_{MSE}	R_{MAE}	G_{MAE}	B_{MAE}	R_{MSE}	$\mathbf{G_{MSE}}$	B_{MSE}	R_{MAE}	G_{MAE}	B_{MAE}	R_{MSE}	$\mathbf{G_{MSE}}$	B_{MSE}
Linear 1	12.06	11.60	12.23	495.83	**468.77**	499.12	16.08	14.55	15.88	922.53	**779.20**	896.20	7.64	6.62	7.63	162.61	**125.83**	165.36
Linear 2	9.75	9.29	10.01	276.85	**248.84**	283.04	11.58	11.22	11.80	493.58	**423.73**	497.45	7.38	6.67	7.59	148.38	**117.85**	155.33
Median 1	7.97	7.49	8.31	241.04	**217.88**	249.27	10.98	9.73	11.11	667.46	**525.80**	651.40	6.41	5.88	6.64	119.66	**96.67**	125.89
Median 2	7.71	7.33	8.07	199.33	**182.68**	206.59	9.55	8.58	9.73	418.99	**330.44**	413.49	6.58	5.96	6.82	120.92	**96.49**	127.18
Median 3	7.30	6.99	7.74	147.81	**133.35**	157.10	8.32	7.50	8.62	243.47	**186.19**	245.85	6.82	6.28	7.15	121.57	**98.70**	129.77
Rational	6.71	6.16	7.04	146.58	**125.82**	155.26	8.63	7.80	8.75	402.53	**341.34**	396.22	5.95	5.39	6.11	113.49	**91.56**	118.59

Table 8: MAE and MSE of all the presented NR methods with the noisy 'Docu'-image.

The results presented in previous tables show the noise reduction capabilities for different kind of test images. It can be seen that the pre-CFAI NR methods with detector can create the smallest error values. Note that, if these results are compared against to the results in Table 2, where the noisy images are interpolated using 'Laplacian2'-method, it can be noticed that these pre-CFAI NR filters can really filter more noise away than the image is smoothed. This is not a case for the post-CFAI filters always. Of course, it is possible to create some kind of detail detector also for the post-CFAI NR methods to improve their results, but the complexity of them is big enough already without it.

3.1 PROCESSING POWER MEASUREMENTS

All the experiments, in this paper, were done using a PC having one 700 MHz Pentium® III processor and Windows NT® 4.0 operating system. Microsoft® Visual C++® 6.0 compiler is used to compile the computer programs, written by authors. Intel VTune™ Performance Analyzer 4.5 is used to measure the runtime of each method. The runtime results by the 'Plant'-image with noise are shown in Table 9.

	Pre	Pre + det.	Post
Linear 1	17	31	48
Linear 2	12	33	47
Median 1	112	116	331
Median 2	50	64	146
Median 3	59	70	167
Rational	120	131	358

Table 9: Processing times of the NR functions in ms.

Method	Time
Pixel Copy	17
Bilinear	24
Hamilton	72
Yuv2rgb	60
Rgb2yuv	75

Table 10: Runtimes of the CFAI methods and color space conversions in ms.

The times presented above can vary a lot, if the processing device or the implementations of filters are changed. Especially, the size of memory and the speed of processor are very critical parameters. Also the optimizer of compiler can made a big difference between the methods. For example, the 'Median 1'-filter has quite big processing time compared to the other median filters. This is due to the fact that the used 5-point median algorithm was not able to be compiled using inline function as the 3-point median algorithm was. Therefore, the results in Table 9 should not be compared too much in vertical direction.

There still are at least two notifications possible to do from the Table 9. The processing time of the post-CFAI NR filter is about three times the processing time of the pre-CFAI NR filter. This was predicted earlier, because the number of processed pixels with the post-CFAI NR filter is also three times the number of processed pixels with the pre-CFAI NR

filter. Also the time used in the pre-CFAI NR detector is something between 10 to 15 ms. For very simple methods, as linear filters, this is quite a lot, but when the method itself takes more time it is not so big proportional addition anymore (e.g. with 'Median 3'-filter about 20 % increase to processing time). Just for comparison, the runtimes of the presented three CFAI methods and the color space conversions are measured by the 'Plant'-image with noise and shown Table 10.

4. CONCLUSIONS

In this paper, some post-CFAI NR and pre-CFAI NR techniques are compared. The effect of different CFAI methods to quality of the result image is also shown. Possibility to reduce more noise with the pre-CFAI NR methods than with the post-CFAI NR methods is shown. Also the processing requirements (e.g. power consumption and size of memory) can be smaller with the pre-CFAI NR methods than with the post-CFAI NR methods. The problem to smooth image with the pre-CFAI NR method has been noticed. Therefore, the new solution for improving the detail preserving properties of the pre-CFAI NR filters is proposed. When using the proposed simple detail detector with limiter, also the level of sharpness provided by the post-CFAI NR methods could be maintained or even improved with the pre-CFAI NR methods.

REFERENCES

1. P. Wallich, "Mindstorms: not just a kid's toy", IEEE Spectrum , vol. 38, issue 9, pp. 52 -57, Sept. 2001.
2. K.-B. Cho, A. Krymski, and E. R. Fossum, "A 1.2 V micropower CMOS active pixel image sensor for portable applications", Digest of Technical Papers of IEEE International Solid-State Circuits Conference, pp. 114 –115, 2000.
3. B. Ackland, and A. Dickinson, "Camera on a chip", Digest of Technical Papers of 42nd IEEE International Solid-State Circuits Conference, pp. 22 -25, 412, 1996.
4. D. S. Messing, and M. I. Sezan, "Improved multi-image resolution enhancement for colour images captured by single-CCD cameras", Proceedings of International Conference on Image Processing, vol. 3, pp. 484 –487, 2000.
5. A. Bosco, and M. Mancuso, "Adaptive filtering for image denoising", Proceedings of International Conference on Consumer Electronics, pp. 208 –209, 2001.
6. A. J. Blanksby, and M. J. Loinaz, "Performance analysis of a color CMOS photogate image sensor", IEEE Transactions on Electron Devices, vol. 47, issue 1, pp. 55 –64, Jan. 2000.
7. S. J. Sangwine, "Colour in image processing", Electronics & Communication Engineering Journal, vol. 12, issue 5, pp. 211 –219, Oct. 2000.
8. J. F. Hamilton, Jr. and J. E. Adams, Jr., "Adaptive Color Plan Interpolation in Single sensor Color Electronic Camera", US patent 5,629,734, May 13, 1997.
9. R. C. Gonzalez, and R. E. Woods, "Digital Image Processing", pp. 191-192, Addison-Wesley Publishing Company, Inc, 1992.
10. W.-S. Lu, and A. Antoniou , "Two Dimensional Digital Filters", pp. 361- 364, Marcel Dekker, Inc. New York, 1992.
11. J. Astola, and P. Kuosmanen, "Fundamentals of Nonlinear Digital Filtering", pp. 88-105, CRC Press LLC, 1997.
12. I. Pitas, and A. N. Venetsanopoulos, "Nonlinear Digital Filters – Principles and Applications", pp. 63 – 150, Kluwer Academic Publishers, Massachusetts, 1991.
13. G. R. Arce, and R. E. Foster, "Multilevel median filters: properties and efficacy", Proceedings of International Conference on Acoustics, Speech, and Signal Processing, vol.2, pp. 824 –827, 1988.
14. G. R. Arce, and R. E. Foster, "Detail-Preserving Ranked-Order Based Filters for Image Processing", IEEE trans. on Acoustics, Speech, and Signal Processing, vol. 37, no. 1, pp. 83 – 98, January 1989.
15. L. Khriji, and M. Gabbouj, " Median-rational hybrid filters", Proceedings of International Conference on Image Processing, vol. 2, pp. 853 –857, 1998.

Image Page 1: Subsampled (320 x 240) images from (640 x 480) originals.

a) 'Plant'

b) 'Tiger'

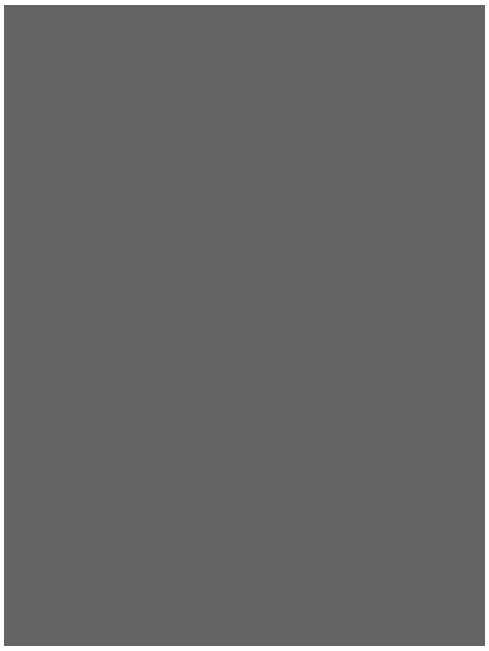

c) 'Gray'

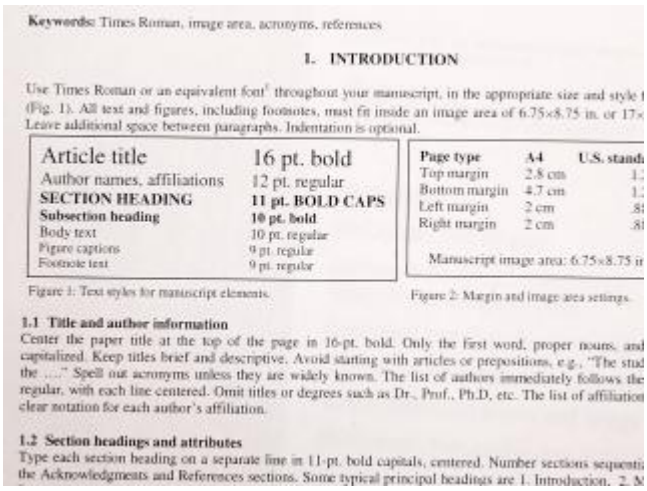

Keywords: Times Roman, image area, acronyms, references

1. INTRODUCTION

Use Times Roman or an equivalent font[1] throughout your manuscript, in the appropriate size and style
(Fig. 1). All text and figures, including footnotes, must fit inside an image area of 6.75×8.75 in. or 17×
Leave additional space between paragraphs. Indentation is optional.

Article title	16 pt. bold
Author names, affiliations	12 pt. regular
SECTION HEADING	**11 pt. BOLD CAPS**
Subsection heading	**10 pt. bold**
Body text	10 pt. regular
Figure captions	9 pt. regular
Footnote text	9 pt. regular

Figure 1: Text styles for manuscript elements.

Page type	A4	U.S. stand
Top margin	2.8 cm	1.
Bottom margin	4.7 cm	1.
Left margin	2 cm	.8
Right margin	2 cm	.8

Manuscript image area: 6.75×8.75 i

Figure 2: Margin and image area settings.

1.1 Title and author information

Center the paper title at the top of the page in 16-pt. bold. Only the first word, proper nouns, and
capitalized. Keep titles brief and descriptive. Avoid starting with articles or prepositions, e.g., "The stud
the ...." Spell out acronyms unless they are widely known. The list of authors immediately follows the
regular, with each line centered. Omit titles or degrees such as Dr., Prof., Ph.D, etc. The list of affiliation
clear notation for each author's affiliation.

1.2 Section headings and attributes

Type each section heading on a separate line in 11-pt. bold capitals, centered. Number sections sequenti
the Acknowledgments and References sections. Some typical principal headings are 1. Introduction, 2. M

d) 'Docu'

Image Page 2: Cropped (160 x 120) image from 'Docu', up-left location (20, 92).

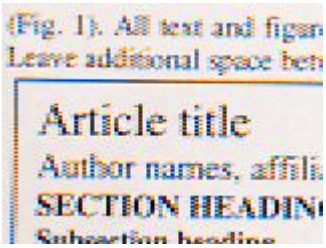

a) Pixel copy CFAI

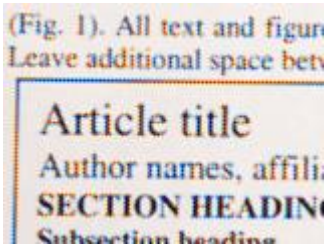

b) Bilinear CFAI

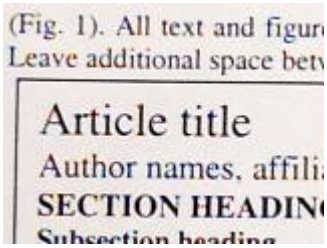

c) Laplacian 2 CFAI

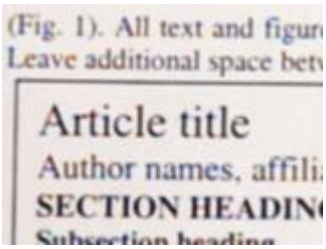

d) Post Linear 1 NR

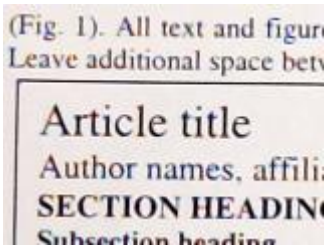

e) Post Median 3 NR

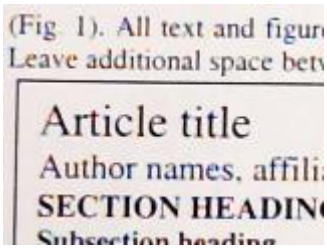

f) Post Rational NR

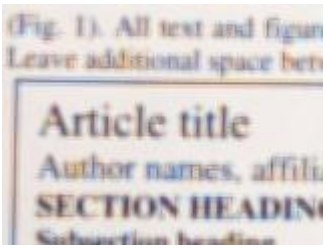

g) Pre Linear 1 NR

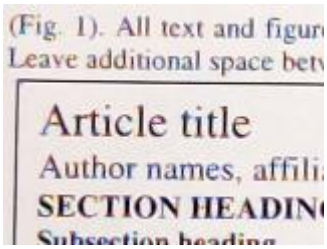

h) Pre Median 3 NR

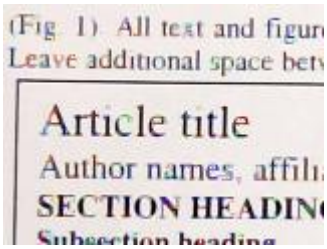

i) Pre Rational NR

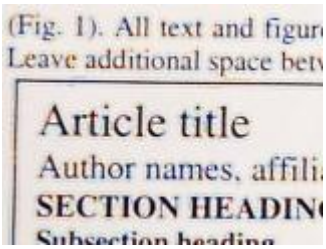

j) Pre Linear 1 NR with detector

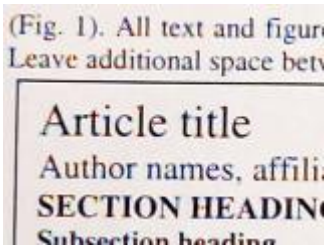

k) Pre Median 3 NR with detector

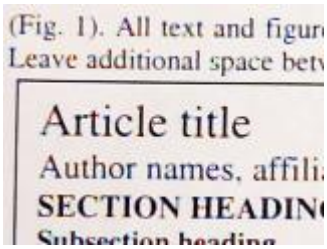

l) Pre Rational NR with detector

Image Page 3: Cropped (160 x 150) image from 'Plant' , up-left location (220, 90).

a) Pixel copy CFAI

b) Bilinear CFAI

c) Laplacian 2 CFAI

d) Post Linear 2 NR

e) Post Median 2 NR

f) Post Rational NR

g) Pre Linear 2 NR

h) Pre Median 2 NR

i) Pre Rational NR

j) Pre Linear 2 NR with detector

k) Pre Median 2 NR with detector

l) Pre Rational NR with detector